Extract of Plastrum Testudinis through miR-214 mediated Wnt/β-catenin signaling stimulating bone formation

Qing Lin
Jinan University
Yumei Yang
Jinan University
Xiaoyun Li (402574826@qq.com)
Jinan University
Haoyu Wang
Jinan University
Yan Cui
Jinan University
Panpan Wang
Jinan University
Xiaofeng Zhu
Jinan University
Li Yang
Jinan University
Ronghua Zhang
Jinan University

Research Article

Keywords: Osteoporosis, Plastrum Testudinis, miR-214, Bone mesenchymal stem cell, bone formation

Posted Date: October 28th, 2022

DOI: https://doi.org/10.21203/rs.3.rs-2202532/v1

Abstract

Plastrum Testudinis (PT) is known as Traditional Chinese Medicine, which has commonly been used to treat and prevent bone metabolism for many years. However, the pharmacological mechanisms have not yet been fully clarified. In this study, we constructed a bilateral ovariectomy model to simulate postmenopausal osteoporosis (OP), then performed intragastric administration of different doses (160, 80, 40 mg/kg/day) of PT for 10 weeks. After treatment, we used dual-energy X-ray absorptiometry to evaluate bone mineral density, and micro-computed tomography and hematoxylin and eosin staining to analyze bone microstructure, immunochemistry, western blotting and quantitative polymerase chain reaction to detect the expression of osteogenic differentiation-related factors; and miRNA over-expression to evaluate the effect of miR-214 on the differentiation of bone mesenchymal stem cells (BMSCs) and related target genes. PT moderated bone mass and bone microstructure, alleviated body weight, and exhibited no estrogen-like effects; promoted the expression of osteogenic differentiation factors in the femur and lumbar vertebrae, as well as facilitated the expression of the Wnt signaling-related factors LRP5, Wnt3a, GSK-3β, and β-catenin. In addition, miR-214 inhibited osteogenic differentiation of BMSCs and targeted the Wnt signaling-related factors Wnt3a and β-catenin, while PT ameliorated these effects. This study indicated that PT may act as an antagonist of miR-214 to stimulate bone formation through β-catenin-mediated Wnt signaling.

1. Introduction

Osteoporosis (OP) is a common clinical bone disease, and postmenopausal women are at particularly high risk. Research has indicated that various factors lead to OP, but insufficient bone formation is one of the most crucial reasons [1]. Bone mesenchymal stem cells (BMSCs) are multipotent cells whose fate of osteogenic differentiation is essential to the process of bone formation [2]. Research has shown that this process is controlled by a variety of factors, including signaling pathways and non-coding RNA [3]. Therefore, figuring out the specific relationship or mechanism among these factors is necessary to better understand the process.

Plastrum Testudinis (PT) is known as Traditional Chinese Medicine which commonly is used as the component in anti-osteoporosis in the Chinese medicine prescription, as well as in tonic foods such as Plastri Testudinis and tortoise jelly. PT could tonify kidney and strengthen bone approved by the Chinese Pharmacopoeia (2020) edition, and the modern research has been demonstrated that it is beneficial to muscular and skeletal development. For instance, PT has the ability to promote neural stem cell differentiation, stimulate skin wound healing [4], promote the proliferation and osteogenic differentiation of BMSCs [5], and alleviate the loss of bone mass and structure in senile or glucocorticoid-induced spinal OP [6, 7]. Although the effects and mechanisms of PT have been explored in different ways, the ability of PT to protect against bone loss in ovariectomized rats, and the specific mechanisms involved, need to be explored further.

Wnt signaling is one of the most significant classical pathways in osteogenic differentiation of BMSCs [8]. Various studies have shown that Wnt, a member of the secretory lipid modification signaling glycoprotein family, participates in bone formation and the process of osteogenic differentiation into osteocytes [9]. Wang et al. [10] indicated that total glycosides and polysaccharides of *Cistanche Deserticola* prevented OP by activating Wnt/β-catenin signaling. Chaetocin has been shown to promote osteogenic differentiation by modulating Wnt/β-catenin signaling in mesenchymal stem cells [11]. Furthermore, the components of the Wnt signaling pathway are regulated by several micro RNAs (miRNAs) [12]. Therefore, more research is needed to elucidate the specific mechanism and efficacy of Wnt in the process of bone remodeling.

In this study, we constructed an ovariectomized rat model to simulate the situation of postmenopausal OP, and evaluated the effects of different doses of PT on bone quality and quantity in ovariectomized rats and BMSCs, as well as exploring the specific mechanism among PT, Wnt signaling, and miR-214. This research may provide a new perspective of PT how to regulate bone metabolism.

2. Results

2.1 PT alleviated a gain in body weight and moderated morphology in OVX rats

Qualitative and relative quantitative analyze of the amino acid constituents including detection of indispensable amino acids and essential amino acids, which we detected before [13]; and the trace elements were determined by coupled plasma emission spectrometer, including sodium, calcium, ferric and so on (Table 1). We then evaluated the effects of PT on ovariectomized rats. It revealed that body weight was higher in OVX rats than sham rats, and supplementation with either PT-H or PT-L significantly reduced the weight gain in OVX rats (Fig. 1a). The weight of the uterus and the uterine index revealed that both were lower in OVX rats than in the Sham group (Fig. 1b), while morphology showed that the uterus was atrophied and thinner in the OVX rats, and different doses of PT caused slight modulation of this effect but without resulting in a significant difference (Fig. 1c). The content of body fat was higher in the OVX rats than the Sham group, and the BMI slightly increased but without a substantial difference; PT-M significantly decreased it in the OVX rats, and different doses of PT slightly reduced the BMI but without causing a noticeable difference (Fig. 1d).

Table 1
The content of trace elements in the PT

Trace element	Average content(ppm mg/L)	RSD(%)	concentration(mg/kg)
B	0.111	0.70	414.1791
Ca	2.557	0.50	9541.045
Cu	0.003	0.10	11.19403
Cr	0.119	0.40	444.0299
Fe	0.243	0.80	906.7164
K	0.55	0.40	2052.239
Ni	0.093	0.30	347.0149
P	0.051	1.50	190.2985
Zn	0.063	0.40	235.0746
Li	0.213	5.00	794.7761
Na	5.817	0.40	21705.22
Mg	0.709	0.30	2645.522
Sr	0.019	2.30	70.89552
Ba	0.009	3.40	33.58209
Al	0.119	0.90	444.0299

2.2 PT increased bone mass and regulated bone turnover biomarkers in OVX rats

The BMD of the whole body, lumbar vertebrae and femur were all lower in the OVX rats than in the Sham rats. PT-H significantly increased the bone mass of the femur in the OVX rats, while the other doses also slightly increased the bone mass at different sites but the difference did not reach significant difference (Fig. 2a). Furthermore, the level of BGP in serum was obviously decreased, while serum PTH levels significantly increased in the OVX rats compared with the Sham group, and PT-M down-regulated serum PTH in OVX rats, but the effect of PT on BGP was not significant (Fig. 2b).

2.3 PT ameliorated bone microstructure in OVX rats

The femur trabeculae appeared irregular, porous and fractured in the OVX rats, with lower BV/TV, Tb.N, and Tb.Th than the Sham group, and the lumbar vertebrae showed the same trend with the exception of Tb.Th which exhibited no significant difference between the Sham and OVX groups (Fig. 3a). Different doses of PT significantly increased the Tb.Sp, and slightly increased the BV/TV and Tb.Th, although there was no significant difference in either the femur or lumbar vertebrae. PT-M and PT-L both

significantly increased the femur Tb.N, while PT-H and PT-M increased the Tb.N of lumbar vertebrae (Fig. 3b). Furthermore, HE staining of the femur and lumbar vertebrae revealed that OVX rats had more sparse and irregular trabeculae than OVX rats; simultaneously, different PT doses moderated these effects (Fig. 3c, 3d).

2.4 PT stimulated expression of osteogenic differentiation-related factors in OVX rats

In the femur, the results indicated that the protein expression of osteogenic-related factors was lower in the OVX group than in the Sham group, while PT-H promoted the expression of ALP, BMP-2, and COL1A1, and PT-M significantly increased the expression of ALP and BMP-2. At the mRNA level, PT-H obviously improved the expression of COL1A1 and Runx2 in OVX rats, PT-M significantly increased the mRNA expression of ALP, BMP-2, COL1A1 and Runx2, and PT-L dramatically increased the expression of BMP-2 and Runx2 (Fig. 4a).In the lumbar vertebrae, both the protein and mRNA expression of osteogenic differentiation-related factors were lower in the OVX group than in the Sham group, while different doses of PT significantly increased the protein expression of ALP, BMP-2, COL1A1 and Runx2 (Fig. 4b).IHC staining showed that the distribution and expression of COL1A1 was sparse in the femur of OVX rats, while PT-H, PT-M, and PT-L modulated these effects to some degree (Fig. 4c); these trends were also in accordance with those observed in the lumbar vertebrae (Fig. 4d)

2.5 PT promoted osteogenic differentiation through Wnt/β-catenin signaling in BMSCs

We analyzed the protein and mRNA expression of Wnt signaling-related factors in bone tissue. The results showed that the protein levels of GSK-3β, LRP5, Wnt3a and β-catenin were down-regulated in the OVX group. PT-M significantly increased the protein levels of Wnt3a and LRP5, while the other doses of PT also slightly promoted expression of Wnt3a, LRP5, GSK-3β, and β-catenin but without resulting in a significant difference (Fig. 5a).

We also evaluated the osteogenic effect of PT on BMSCs. The results showed that PT significantly promoted the expression of ALP, BMP-2, COL1A1, and Runx2 in BMSCs. We then adopted a classical Wnt signaling inhibitor, Dkk-1, and found that the expression of Wnt3a, LRP5, and β-catenin were all significantly down-regulated in the Dkk-1 group, which meant that Wnt signaling was blocked. Furthermore, compared with the PT group, the expression of BMP-2, Runx2, and COL1A1 was significantly down-regulated in the group treated with a combination of PT and Dkk-1. Analysis of mRNA expression showed the same trend (Fig. 5b).

2.6 PT mediated miR-214 regulation of Wnt signaling to control osteogenesis

A previous study indicated that the expression of miR-214 is negatively related to osteogenesis [14]. We analyzed the expression of miR-214 in bone tissue, and found that miR-214 was obviously increased in

the OVX rats, while PT abated this effect (Fig. 6a); furthermore, the expression of miR-214 was down-regulated simultaneously with osteogenic induction at different timepoints (Fig. 6b). Over-expression of miR-214 showed that osteogenesis-related factors were significantly decreased in the miR-214 mimic group compared with the NC group. Alizarin red S staining supported these results (Fig. 6c, 6d). Analysis by miRbase and Targetscan showed that miR-214 has a strong affinity with β-catenin and Wnt3a (Fig. 6e); in addition, various studies have indicated that miR-214 regulates activation of Wnt signaling. We observed that the miR-214 mimic down-regulated the expression of Wnt signaling components, while PT rescued the effects of miR-214 (Fig. 6f).

3. Methods And Materials

3.1 Preparation of water extraction of PT and component analysis

PT (*Chinemys reevesii*) was purchased from local pharmacies (batch number 18082114). Following a previous study [13], PT was twice extracted by decoction in distilled water (2 h each time), and then concentrated by rotary evaporation to a final concentration of 0.1 g/L. After cooling the extract to room temperature, it was stored at -20°C under dry, airproof, and non-polluted conditions until further use.

Based on the properties of PT, trace elements of the PT extracts were determined by coupled plasma emission spectrometer (Thermo Scientific, X SERIES2), the results were carried out twice in parallel then calculated.

3.2 Animal treatments

Ten-week-old healthy female Sprague Dawley rats were obtained from Guangdong Medical Laboratory Animal Center (SYXK (Yue) 2017 – 0174). All animal procedures were approved by the Animal Care Committee of Jinan University. Rats were allowed a one-week adaptive phase, and then bilateral ovariectomy surgery was conducted according to the technique described in previous studies [13]. The rats were divided into five groups: a sham-operated group (Sham; sham surgery followed by treatment with phosphate buffer), an ovariectomized group (OVX; ovariectomy surgery followed by treatment with phosphate buffer), an ovariectomized group treated with high-dose PT (PT-H; 160 mg/kg/day), an ovariectomized group treated with mid-dose PT (PT-M; 80 mg/kg/day), and an ovariectomized group treated with low-dose PT (PT-L; 40 mg/kg/day) by intragastric administration. The doses of PT treatment for each group were one, two and four times, respectively, the body surface area conversion of clinical doses according to the formula of Chinese medicine. At the time point, rats were sacrificed and samples were collected for further use.

3.3 Hematoxylin and eosin (HE) and immunohistochemical (IHC) analysis

Femurs and lumbar vertebrae were collected and fixed with 4% paraformaldehyde solution, then decalcified with 10% EDTA at room temperature for one month. Afterwards, samples were dehydrated with an alcohol gradient and embedded in paraffin, then cut into 5 μm thick sections. Some of the sections were stained with HE, while others were prepared for IHC analysis. Briefly, the sections were prepared, stained, counterstained, dehydrated, hyalinized, and mounted, then the antibody against COL1A1 (E8F4L, Cell signaling technology, Danvers, MA, USA) was diluted at 1: 100. All images were captured using a microscope (Zeiss, AXIO; Carl Zeiss Microscopy GmbH, Jena, Germany).

3.4 Bone mineral density (BMD) and micro computed tomography (CT) analysis

The BMD of the rats was analyzed by dual-energy X-ray absorptiometry (DXA; GE Healthcare, Pittsburgh, PA, USA), which was loaded with software specific for small animals to assess bone density, bone mineral content (BMC), body fat content, and body mass index (BMI).

Femurs and lumbar vertebrae were fixed in 4% paraformaldehyde, then analyzed using a Hiscan XM Micro CT (Suzhou Hiscan Information Technology Co., Ltd., Soochow, China). The X-ray tube settings were 60 kV and 133 A and images were acquired at 50 m resolution. A 0.5° rotation step through a 360° angular range with 50 ms exposure per step was used. The images were reconstructed with Hiscan Reconstruct software (Version 3.0, Suzhou Hiscan Information Technology Co., Ltd.) and analyzed using Hiscan Analyzer software (Version 3.0, Suzhou Hiscan Information Technology Co., Ltd.). Then, the bone volume/tissue volume (BV/TV), trabecular number (Tb.N), trabecular thickness (Tb.Th), and trabecular separation (Tb.Sp) data were collected.

3.5 Western-blot analyses

Total protein was extracted using RIPA buffer (P0013B, Beyotime Institute of Biotechnology, Jiangsu, China) supplemented with a protease inhibitor cocktail. The protein concentration was then measured using a BCA assay kit (23225, Thermo Fisher Scientific, Waltham, MA, USA) according to the manufacturer's instructions. Protein contained in different samples was separated by sodium dodecyl sulfate polyacrylamide gel electrophoresis and then transferred to a polyvinylidene difluoride membrane. The membrane was then incubated overnight at 4°C with the following primary antibodies: anti-ALP (GTX42809, GeneTex, Irvine, CA, USA), anti-COL1A1 (E8F4L, Cell Signaling Technology, Danvers, MA, USA), anti-RUNX2 (D1H7, Cell Signaling Technology), anti-BMP-2 (ab225898, Abcam, Cambridge, MA, USA), anti-LRP5 (D80F2, Cell Signaling Technology), anti-Wnt3a (C64F2, Cell Signaling Technology), or anti-β-catenin (D10A8, Cell Signaling Technology). On the second day, the membranes were incubated with an HRP-conjugated secondary antibody (1:3000, 7074P2, Cell Signaling Technology) at 37°C for 2 h and finally visualized using an ultra-sensitive luminescent fluid (4A Biotech, Beijing, China). The results were quantified using Image J (NIH, Bethesda, MD, USA).

3.6 Real-time Quantitative Polymerase Chain Reaction

Total RNA was extracted using Trizol reagent (15595-026, Thermo Fisher Scientific), and reverse transcription of mRNA was performed using the PrimeScript RT reagent kit (PR037A, TakaRa Bio Inc., Shiga, Japan), while miRNAs using the miRNA First Strand cDNA Synthesis (Tailing Reaction) (B532451, Shenggong, China). The corresponding primers were synthesized commercially (Shenggong, China) and are listed in Table 2. The cDNA amplification was followed by addition of SYBR Green mix (A302, Genstar, China); GAPDH or U6 was used as an internal reference. All relative gene expression values were calculated using the formula $2^{-\triangle\triangle ct}$.

Table 2
The prime sequences

Gene/miRNAs name	5'-3' sequence	
Bmp-2	Forward:	GCCATCGAGGAACTTTCAGA
	Resverse:	TGTTCCCGAAAAATCTGGAG
Alpl	Forward:	GACAAGAAGCCCTTCACAGC
	Resverse:	ACTGGGCCTGGTAGTTGTTG
Col1a1	Forward:	ACGTCCTGGTGAAGTTGGTC
	Resverse:	TCCAGCAATACCCTGAGGTC
Runx2	Forward:	AACAGCAGCAGCAGCAGCAG
	Resverse:	GCACGGAGCACAGGAAGTTGG
β-catenin	Forward:	GAAAATGCTTGGGTCGCCAG
	Resverse:	ATGGCAGGCTCGGTAATGTC
Lrp5	Forward:	GGACATCGAGTTTGGTGGGA
	Resverse:	GTTGTTGTGGCGGTTCATGG
Wnt3a	Forward:	TGGTGGTGGTGGTGGCAGAG
	Resverse:	CACAGCCAAGGACCAGAGAAGAAC
Lrp5	Forward:	GGACATCGAGTTTGGTGGGA
	Resverse:	GTTGTTGTGGCGGTTCATGG
Gapdh	Forward:	GACATGCCGCCTGGAGAAAC
	Resverse:	AGCCCAGGATGCCCTTTAGT
miR-214	Forward:	GTCCTGGATGGACAGAGTTGTCA
U6	Forward:	CTCGCTTCGGCAGCACATATACT

3.7 Enzyme-linked immunosorbent assay (ELISA)

The content of bone turnover markers including bone gla protein (BGP), estradiol, parathyroid hormone (PTH), and C-terminal telopeptide (CTX) were measured using commercial ELISA kits from eLabscience (Houston, TX, USA).

3.8 Cell culture

Rat BMSCs were obtained from Cyagen Bioscience (Guangzhou, China), and then cultured in α-MEM (Gibco, Carlsbad, CA, USA) containing 10% fetal bovine serum (FBS500-S, Ausgenex Pty, Molindar, Queensland, Australia) at 37°C with 5% CO_2.

3.9 Cell transfection

BMSCs were seeded into 6-well plates and transfected with 50 nM miR-214 mimic. Briefly, once cells reached 70% confluence, they were incubated with 500 μL transfection mix (Lipofectamine 3000; L3000008, Invitrogen, Carlsbad, CA, USA) with corresponding mimic or negative control (NC; RuiBo Biological Technology Co., Ltd, Guangzhou, China) for 48 h at 37°C, after which the mixture was replaced with fresh culture medium for further experiments.

3.10 Alizarin red s staining

BMSCs were seeded into 60 cm culture dishes and cultured with different treatments. Briefly, the culture medium was replaced every two days, then on day 28 of culture, the medium was discarded, and cells were fixed in 75% ethanol for 10 min, washed with phosphate-buffered saline, and stained with 0.1% alizarin red S (G1450, Solarbio, Beijing, China). After staining for approximately 5 min at room temperature, the wells were rinsed to remove excess dye, and three images of each group were captured.

3.11 Data analysis

All experimental values are shown as mean ± standard deviation (SD) or replicate value. Comparisons between groups were analyzed by one-way analysis of variance (ANOVA), the experimental results were analyzed using Graphpad 8.0 software, and the *P* value was considered statistically significant when less than 0.05.

4. Discussion

Osteoporosis is a major public health concern in the older population, with an estimated prevalence of 20.6% in women aged 40 years or older in China [15]. Therefore, it is necessary to search for an effective and safe way to prevent and treat OP, since the existing drugs have different drawbacks and limited clinical usage [16]. Therefore, it is inspiration to find out a drug that have less adverse effects, but also have some positive effect to protect skeleton health [17, 18]. PT is a type of kidney-nourishing medicine which has been used to treat bone disease for many years, and it also known as the main component of health-care products, but the specific mechanism has not been fully elucidated.

In this study, we firstly analyzed the component of the extracts of PT, the results revealed that is abundant in amino acids, such as glycine and glutamic acid, which components have been reported have the effect of anti-osteoporosis [19, 20]; furthermore, the trace element showed that Calcium, Magnesium were the main elements in the Extract of PT, which also participate the process of bone formation and bone absorption [21, 22]. We then evaluated the anti-OP effects of PT. Research had indicated that various anti-OP drugs exert an estrogen-like effect, which results in a high risk of cardiovascular disease and other problems [23, 24]. In this study, we found that OVX rats exhibited no abnormal weight gain or morphological alternations in the uterus following treatment with PT, indicating that PT has no significant estrogen-like effects. We noticed that PT slightly decreased body weight in the OVX rats, together with body fat content and bone mass index. Lu et al. indicated that OVX rats also exhibit accumulation of short-chain fatty acids and produce increased amounts of total bile acids [25]. Fatty tissue is abundant in estrogen receptors, and participates in the secretion of estrogen. Therefore, the accumulation of fatty tissue could compensate for the reduced content of estrogen to some degree [26, 27], which also corresponds to the clinical phenomenon that postmenopausal women have a higher content of abdominal fat [28]. BMD and bone micro-structure are crucial indicators of bone status, and the femur and lumbar vertebrae are places that are especially likely to suffer bone fragility [29]. Our micro CT and BMD results indicated that PT moderated bone mass and bone microstructure in the OVX rats, and HE staining also revealed that the bone trabeculae exhibited more integrity and a more regular structure, while PT also increased the expression of osteogenic differentiation-related factors. Furthermore, the bone turnover marker of PTH was significant down reduced under the treatment of PT-M, while BGP is not obviously, in combination, these results show that PT significantly stimulated bone formation, which is in agreement with the findings of a previous study [30], and the PT-M may work the best.

BMSCs are multi-potential cells located in the bone myeloid. Osteogenic differentiation is crucial to the process of bone formation [31]. Therefore, we next evaluated the effects of different concentrations of PT on BMSCs, which revealed that PT had no significant effect on proliferation, but stimulated osteogenic differentiation, which further confirmed that PT stimulated bone formation. Research has identified various factors that mediate the processes of BMSC differentiation, including signaling pathways, cytokines, as well as non-coding RNA and other factors [32]. Wnt signaling is involved in the process of bone metabolism, as has been proved several times, with cytoplasmic β-catenin entering the nucleus and recruiting transcriptional coactivators and histone modifiers, promoting transcription of target genes [33, 34]. In this study, we found that PT significantly rescued the expression of Wnt-related factors that were down-regulated in OVX rats, as well as rescuing the expression that was inhibited by Dkk-1. Therefore, activation of Wnt signaling is necessary for PT to stimulate bone formation.

miRNA is a type of non-coding RNA, which has been shown to participate in bone formation and bone resorption. A previous study has indicated that miR-214 attenuates osteogenic differentiation of mesenchymal stem cells [35], increases osteoclasts activity and reduces bone mineral density [36]. In this study, we found that miR-214 was down-regulated during osteogenic induction at different time points, which corresponds to the result that miR-214 negatively regulates osteogenesis [37]. Subsequent experiments indicated that PT attenuated the expression of miR-214 in bone tissue. We then considered

whether there was any correlation between Wnt and miR-214. Studies indicated that miR-214 inhibits differentiation of human mesenchymal stem cells into osteoblasts by targeting β-catenin [38], and that miRNA-214 promotes 3T3-L1 preadipocyte differentiation by interfering with the Wnt/β-catenin signaling pathway [14]. Furthermore, Targetscan and miRbase software indicated that one of the target genes of miR-214 is β-catenin, which is a crucial factor in the Wnt signaling pathway. Therefore, we wondered whether PT stimulated bone formation through the Wnt signaling pathway. The results showed that PT significantly down-regulated the expression of miR-214 in OVX rats. Further miR-214 over-expression experiments showed that PT rescued expression of Wnt signaling-related genes in BMSCs. Therefore, we are the first time to report a traditional Chinese medicine may act as an antagonist of miR-214 to stimulate bone formation. The limitation of this work is not specifically explained which component is more important in the extract of PT. Maybe, in the future work, we can evaluate the specific amino or trace element effects on bone metabolism.

Conclusion

This study indicated that PT may act as an antagonist of miR-214 to stimulate bone formation through β-catenin-mediated Wnt signaling. In general, this research explained the specific mechanism of PT as the main component of health products to regulate bone metabolism.

Declarations

Authors' Contributions

Ronghua Zhang and Xiaoyun Li designed and conducted the whole experiment, Qing Lin, Yumei Yang and Xiaoyun Li completed most of the experiments and drafted the manuscript, Yan Cui, Panpan Wang, Haoyu Wang, Li Yang and Xiaofeng Zhu assisted the measurement of related parameters and revised the manuscript.

Funding

This work was supported by the national natural science foundation of China (grant No. 81873202, 81973717 and 82074287), National Key R&D Program of China (No. 2018YFC2002500), National Natural Science Foundation of Guangdong Province (No. 2020A1515010645), Guangdong Provincial Key laboratory of Traditional Chinese Medicine Informatization (2021B1212040007) and Fundamental Research Funds for the Central Universities (21622329). The authors would like to express their gratitude to Analytical and Testing Center of Jinan University for research equipment and technical support for this research.

Data Availability

All data are available from the corresponding author on request.

Compliance with ethical standards

Conflicts of Interest All authors declare that they have no conflict of interest.

References

1. Wang L, You X, Zhang L, Zhang C, Zou W (2022) Mechanical regulation of bone remodeling. Bone Res 10(1):16
2. Infante A, Rodríguez CI (2018) Osteogenesis and aging: lessons from mesenchymal stem cells. Stem Cell Res Ther 9(1):244
3. Sima LE (2017) Extracellular Signals for Guiding Mesenchymal Stem Cells Osteogenic Fate. Curr Stem Cell Res Ther 12(2):139–144
4. Tang Y, Chun LI, Xiangjun LI, Yuqiong WU, Zhang S, Chen D (2017) Study on Plastrum Testudinis Extracts in Promoting Skin Wound Healing through Activating Wnt/ beta-catenin Signaling Pathway. Traditional Chinese Drug Research And Clinical Pharmacology 28(3):171–176
5. Shang Q, Yu X, Ren H, Shen G, Zhao W, Zhang Z, Huang J, Yu P, Liang D, Tang J, Jiang X (2019) Effect of Plastrum Testudinis Extracts on the Proliferation and Osteogenic Differentiation of rBMSCs by Regulating p38 MAPK-Related Genes. Evid Based Complement Alternat Med 2019: 6815620
6. Liang D, Ren H, Qiu T, Shen G, Xie B, Wei Q, Yao Z, Tang J, Zhang Z, Jiang X (2016) Extracts from plastrum testudinis reverse glucocorticoid-induced spinal osteoporosis of rats via targeting osteoblastic and osteoclastic markers. Biomed Pharmacother 82:151–160
7. Zhang P, Chen H, Shen G, Zhang Z, Yu X, Shang Q, Zhao W, Li D, Li P, Chen G, Liang D, Jiang X, Ren H (2021) Network pharmacology integrated with experimental validation reveals the regulatory mechanism of plastrum testudinis in treating senile osteoporosis. J Ethnopharmacol 276:114198
8. Houschyar KS, Tapking C, Borrelli MR, Popp D, Duscher D, Maan ZN, Chelliah MP, Li J, Harati K, Wallner C, Rein S, Pförringer D, Reumuth G, Grieb G, Mouraret S, Dadras M, Wagner JM, Cha JY, Siemers F, Lehnhardt M, Behr B (2019) Wnt Pathway in Bone Repair and Regeneration - What Do We Know So Far. Front Cell Dev Biol 6:170
9. Maeda K, Kobayashi Y, Koide M, Uehara S, Okamoto M, Ishihara A, Kayama T, Saito M, Marumo K (2019) The Regulation of Bone Metabolism and Disorders by Wnt Signaling. Int J Mol Sci 20(22):5525
10. Wang F, Tu P, Zeng K, Jiang Y (2021) Total glycosides and polysaccharides of Cistanche deserticola prevent osteoporosis by activating Wnt/β-catenin signaling pathway in SAMP6 mice. J Ethnopharmacol 271:113899
11. Liang Y, Liu X, Zhou R, Song D, Jiang YZ, Xue W (2021) Chaetocin Promotes Osteogenic Differentiation via Modulating Wnt/Beta-Catenin Signaling in Mesenchymal Stem Cells. Stem Cells Int 2021:8888416
12. Song JL, Nigam P, Tektas SS, Selva E (2015) microRNA regulation of Wnt signaling pathways in development and disease. Cell Signal 27(7):1380–1391

13. Li X, Cui Y, Lin Q, Wang P, Chen R, Zhu X, Yang L, Zhang R (2021) miR-330-5p in Small Extracellular Vesicles Derived From Plastrum testudinis-Preconditioned Bone Mesenchymal Stem Cells Attenuates Osteogenesis by Modulating Wnt/beta-Catenin Signaling. Front Mol Biosci 8:679345
14. Xi FX, Wei CS, Xu YT, Ma L, He YL, Shi XE, Yang GS, Yu TY (2019) MicroRNA-214-3p Targeting Ctnnb1 Promotes 3T3-L1 Preadipocyte Differentiation by Interfering with the Wnt/-Catenin Signaling Pathway. Int J Mol Sci 20(8):1816
15. Wang L, Yu W, Yin X, Cui L, Tang S, Jiang N, Cui L, Zhao N, Lin Q, Chen L, Lin H, Jin X, Dong Z, Ren Z, Hou Z, Zhang Y, Zhong J, Cai S, Liu Y, Meng R, Xia W (2021) Prevalence of Osteoporosis and Fracture in China The China Osteoporosis Prevalence Study. JAMA Netw Open 4(8): e2121106
16. Noh JY, Yang Y, Jung H (2020) Molecular Mechanisms and Emerging Therapeutics for Osteoporosis. Int J Mol Sci 21(20):7623
17. Ni J, Au M, Kong H, Wang X, Wen C (2021) Lycium barbarum polysaccharides in ageing and its potential use for prevention and treatment of osteoarthritis: a systematic review. BMC Complement Med Ther 21(1):212
18. Zhao P, Zhao C, Li X, Gao Q, Huang L, Xiao P, Gao W (2018) The genus Polygonatum: A review of ethnopharmacology, phytochemistry and pharmacology. J Ethnopharmacol 214:274–291
19. Zhou X, Cornel EJ, Fan Z, He S, Du J (2021) Bone-Targeting Polymer Vesicles for Effective Therapy of Osteoporosis. Nano Lett 21(19):7998–8007
20. Li X, Lin Q, Cui Y, Wang H, Wang P, Yang L, Ye Q, Zhang R, Zhu X (2022) Glycine Acts Through Estrogen Receptor Alpha to Mediate Estrogen Receptor Signaling, Stimulating Osteogenesis and Attenuating Adipogenesis in Ovariectomized Rats. Mol Nutr Food Res 66(11):e2100857
21. Liu C, Kuang X, Li K, Guo X, Deng Q, Li D (2020) Effects of combined calcium and vitamin D supplementation on osteoporosis in postmenopausal women: a systematic review and meta-analysis of randomized controlled trials. Food Funct 11(12):10817–10827
22. He B, Xia L, Zhao J, Yin L, Zhang M, Quan Z, Ou Y, Huang W (2021) Causal Effect of Serum Magnesium on Osteoporosis and Cardiometabolic Diseases. Front Nutr 8:738000
23. Skjødt MK, Frost M, Abrahamsen B (2019) Side effects of drugs for osteoporosis and metastatic bone disease. Br J Clin Pharmacol 85(6):1063–1071
24. Li L, Gong M, Bao D, Sun J, Xiang Z (2020) Denosumab and romosozumab do not increase the risk of cardiovascular events in patients with primary osteoporosis: A reanalysis of the meta-analysis. Bone 134:115270
25. Lu H, Gui Y, Guo T, Wang Q, Liu X (2015) Effect of the particle size of cellulose from sweet potato residues on lipid metabolism and cecal conditions in ovariectomized rats. Food Funct 6(4):1185–1193
26. Kim JH, Cho HT, Kim YJ (2014) The role of estrogen in adipose tissue metabolism: insights into glucose homeostasis regulation. Endocr J 61(11):1055–1067
27. Lakoski SG, Herrington DM (2005) Effects of oestrogen receptor-active compounds on lipid metabolism. Diabetes Obes Metab 7(5):471–477

28. Ambikairajah A, Walsh E, Cherbuin N (2019) Lipid profile differences during menopause: a review with meta-analysis. Menopause 26(11):1327–1333
29. Kim MY, Lee K, Shin HI, Lee KJ, Jeong D (2021) Metabolic activities affect femur and lumbar vertebrae remodeling, and anti-resorptive risedronate disturbs femoral cortical bone remodeling. Exp Mol Med 53(1):103–114
30. Shen GY, Ren H, Huang JJ, Zhang ZD, Zhao WH, Yu X, Shang Q, Qiu T, Zhang YZ, Tang JJ, Liang D, Yang ZD, Jiang XB (2018) Plastrum Testudinis Extracts Promote BMSC Proliferation and Osteogenic Differentiation by Regulating Let-7f-5p and the TNFR2/PI3K/AKT Signaling Pathway. Cell Physiol Biochem 47(6):2307–2318
31. Khan AU, Qu R, Fan T, Ouyang J, Dai J (2020) A glance on the role of actin in osteogenic and adipogenic differentiation of mesenchymal stem cells. Stem Cell Res Ther 11(1):283
32. Hu L, Yin C, Zhao F, Ali A, Ma J, Qian A (2018) Mesenchymal Stem Cells: Cell Fate Decision to Osteoblast or Adipocyte and Application in Osteoporosis Treatment. Int J Mol Sci 19(2):360
33. Oichi T, Otsuru S (2020) Wnt signaling in chondroprogenitors during long bone development and growth. Bone 137:115368
34. Taipaleenmäki H (2018) Regulation of Bone Metabolism by microRNAs. Curr Osteoporos Rep 16(1):1–12
35. Yang L, Ge D, Cao X, Ge Y, Chen H, Wang W, Zhang H (2016) MiR-214 Attenuates Osteogenic Differentiation of Mesenchymal Stem Cells via Targeting FGFR1. Cell Physiol Biochem 38(2):809–820
36. Zhao C, Sun W, Zhang P, Ling S, Li Y, Zhao D, Peng J, Wang A, Li Q, Song J, Wang C, Xu X, Xu Z, Zhong G, Han B, Chang YZ, Li Y (2015) miR-214 promotes osteoclastogenesis by targeting Pten/PI3k/Akt pathway. RNA Biol 12(3):343–353
37. Sun Y, Kuek V, Liu Y, Tickner J, Yuan Y, Chen L, Zeng Z, Shao M, He W, Xu J (2018) MiR-214 is an important regulator of the musculoskeletal metabolism and disease. J Cell Physiol 234(1):231–245
38. Li JP, Zhuang HT, Xin MY, Zhou YL (2017) MiR-214 inhibits human mesenchymal stem cells differentiating into osteoblasts through targeting beta-catenin. Eur Rev Med Pharmacol Sci 21(21):4777–4783

Figures

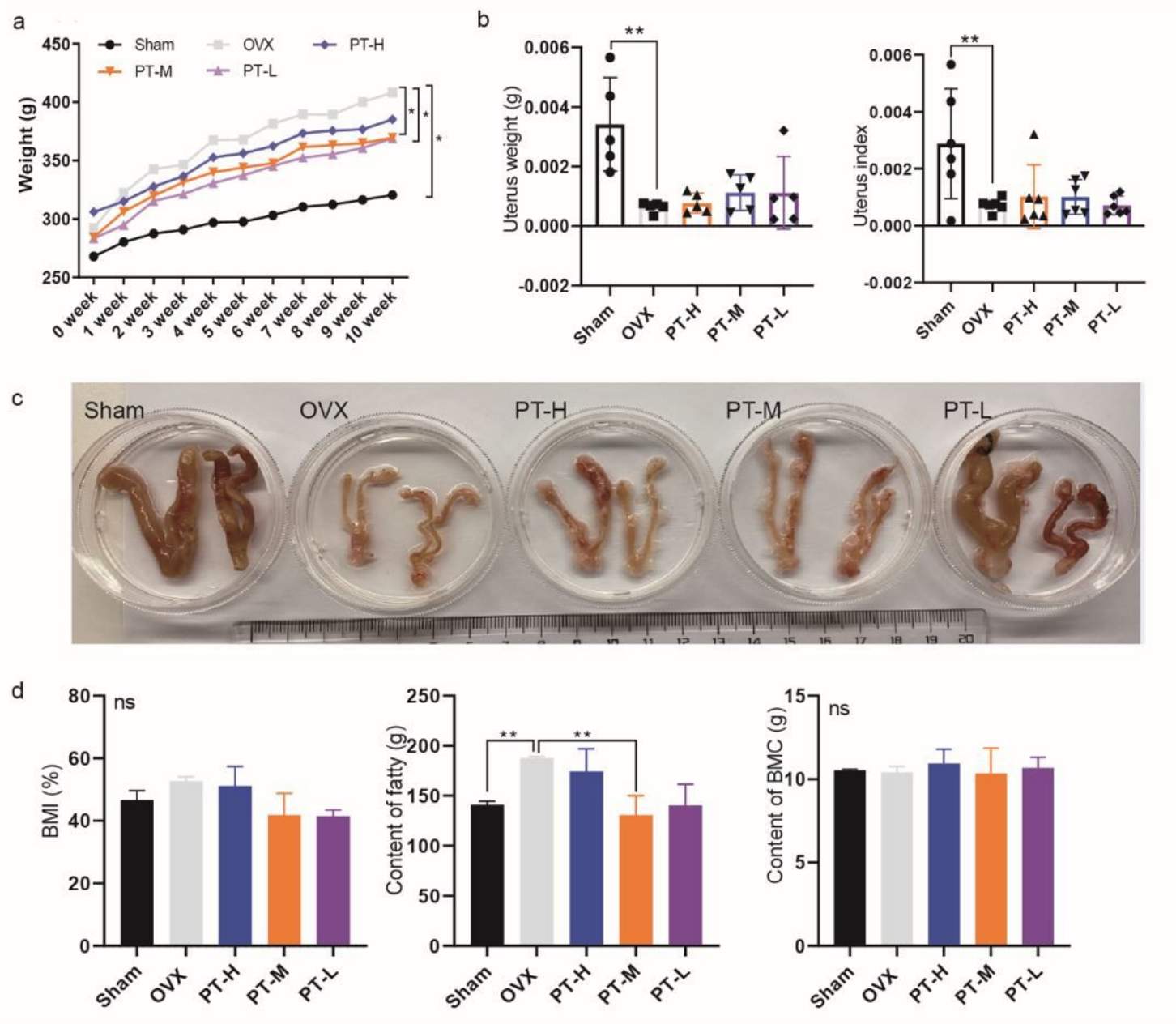

Figure 1

The body weight, uterine status, BMI, BMC, and body fat content of rats. (a) Curve representing the change in body weight (*n*= 6), the raw data represent replicate values; (b) uterine weight and index (*n*= 5), the raw data represent replicate values; (c) uterine morphology (*n*= 2); (d) BMI, body fat content, and content of BMC in different groups (*n*= 4), the raw data represent replicate values. ** $P < 0.01$, ns: not significant, analyses were carried out twice and comparable results were obtained.

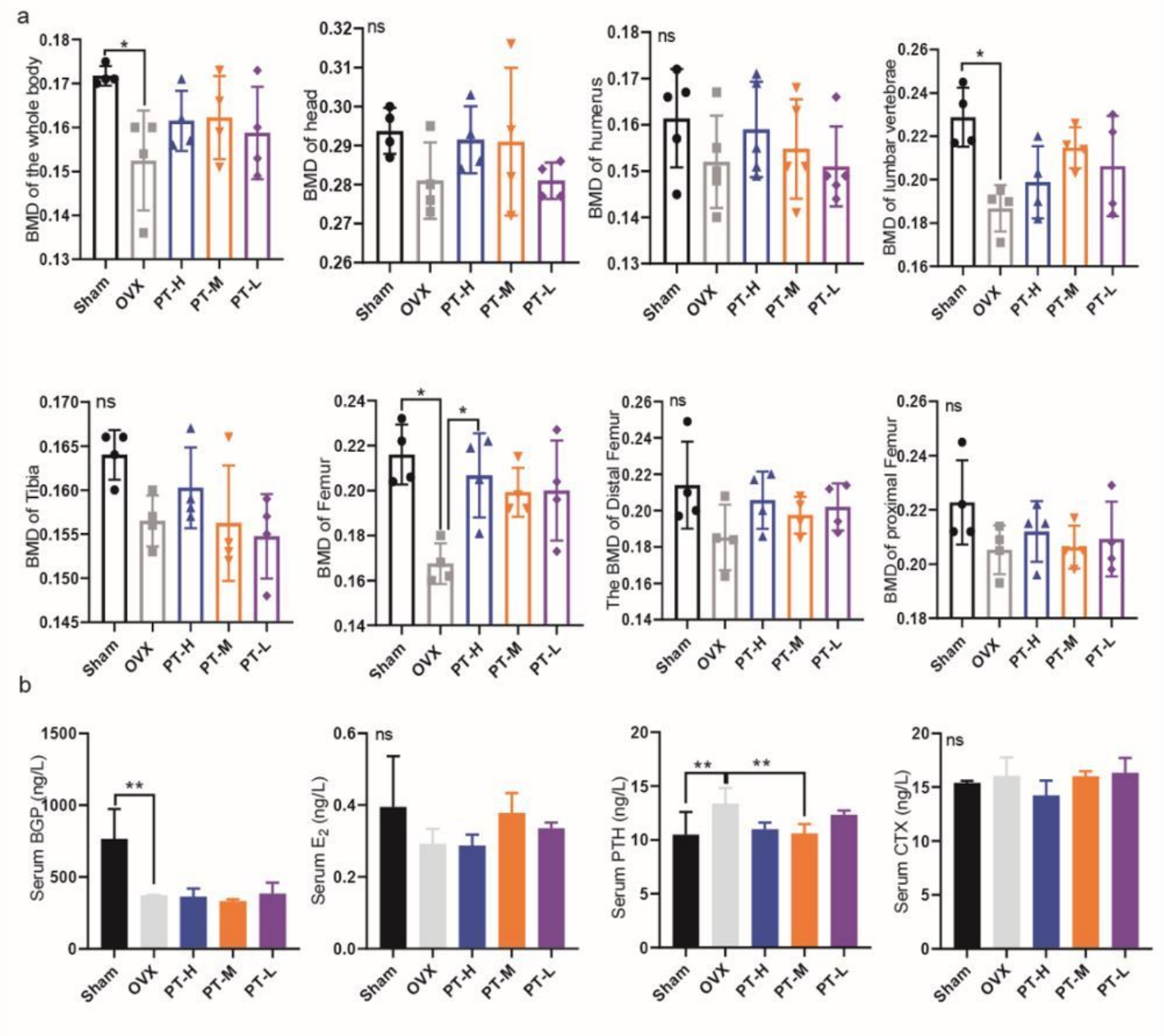

Figure 2

BMD and bone turnover biomarkers in the different experimental groups. (a) BMD of different sites in the different experimental groups (n = 4), the raw data represent replicate values; (b) the content of bone turnover biomarkers in serum of rats in the different experimental groups (n = 5), the raw data represent replicate values.

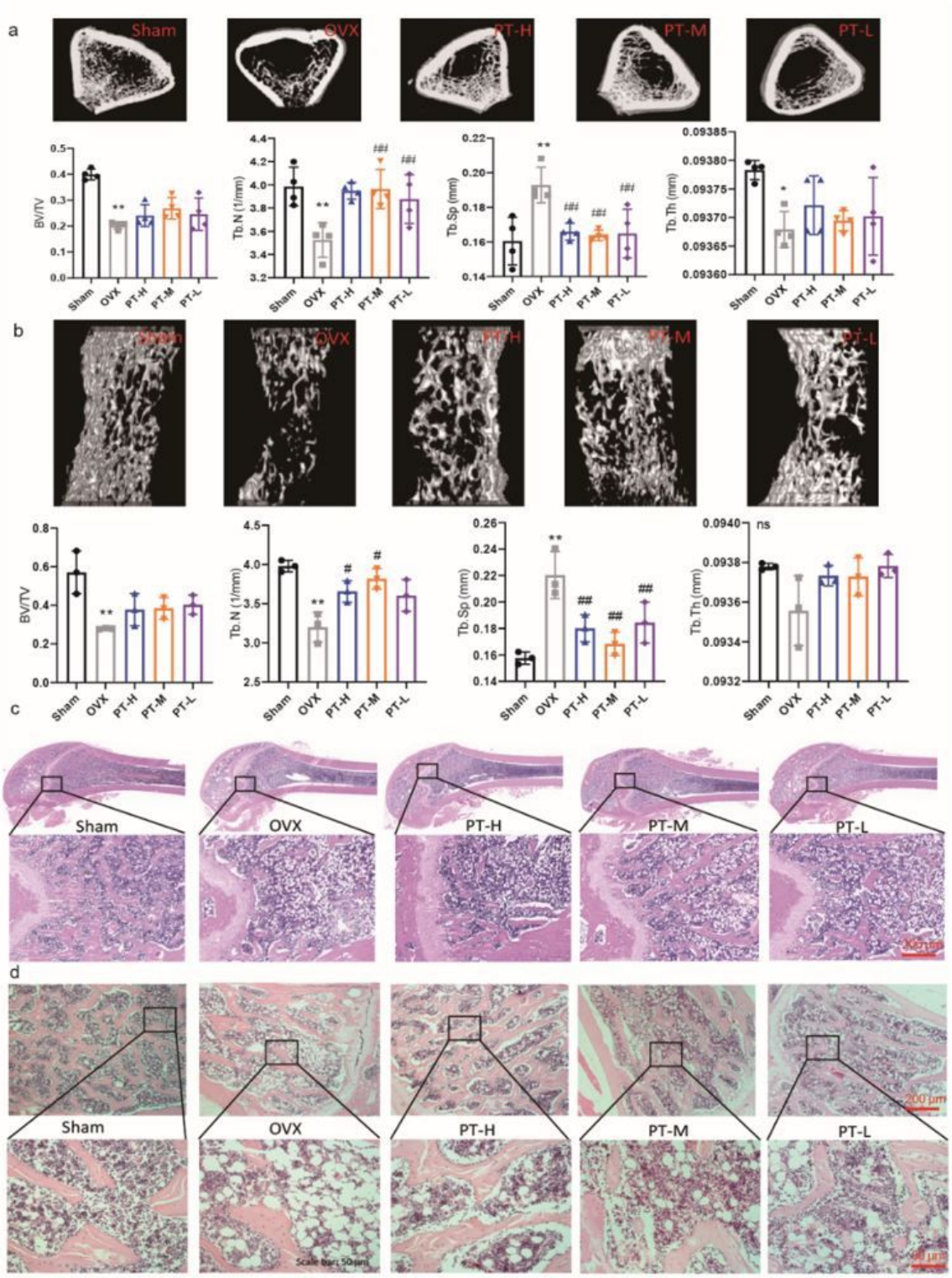

Figure 3

Bone microstructure of the femur and lumbar vertebrae in the different experimental groups. (a) Micro CT of the femur (n = 4), the raw data represent replicate values; (b) micro CT of the lumbar vertebrae (n = 3), the raw data represent replicate values; (c) HE staining of the femur, scale bar: 200 μm; (d) HE staining of the lumbar vertebrae, scale bar: 50 μm or 200 μm. *P < 0.05 vs Sham, **P < 0.01 vs Sham; $^{\#}P$ < 0.05 vs

OVX, $^{\#\#}P < 0.01$ vs OVX, ns: not significant. All analyses were performed twice and comparable results were obtained.

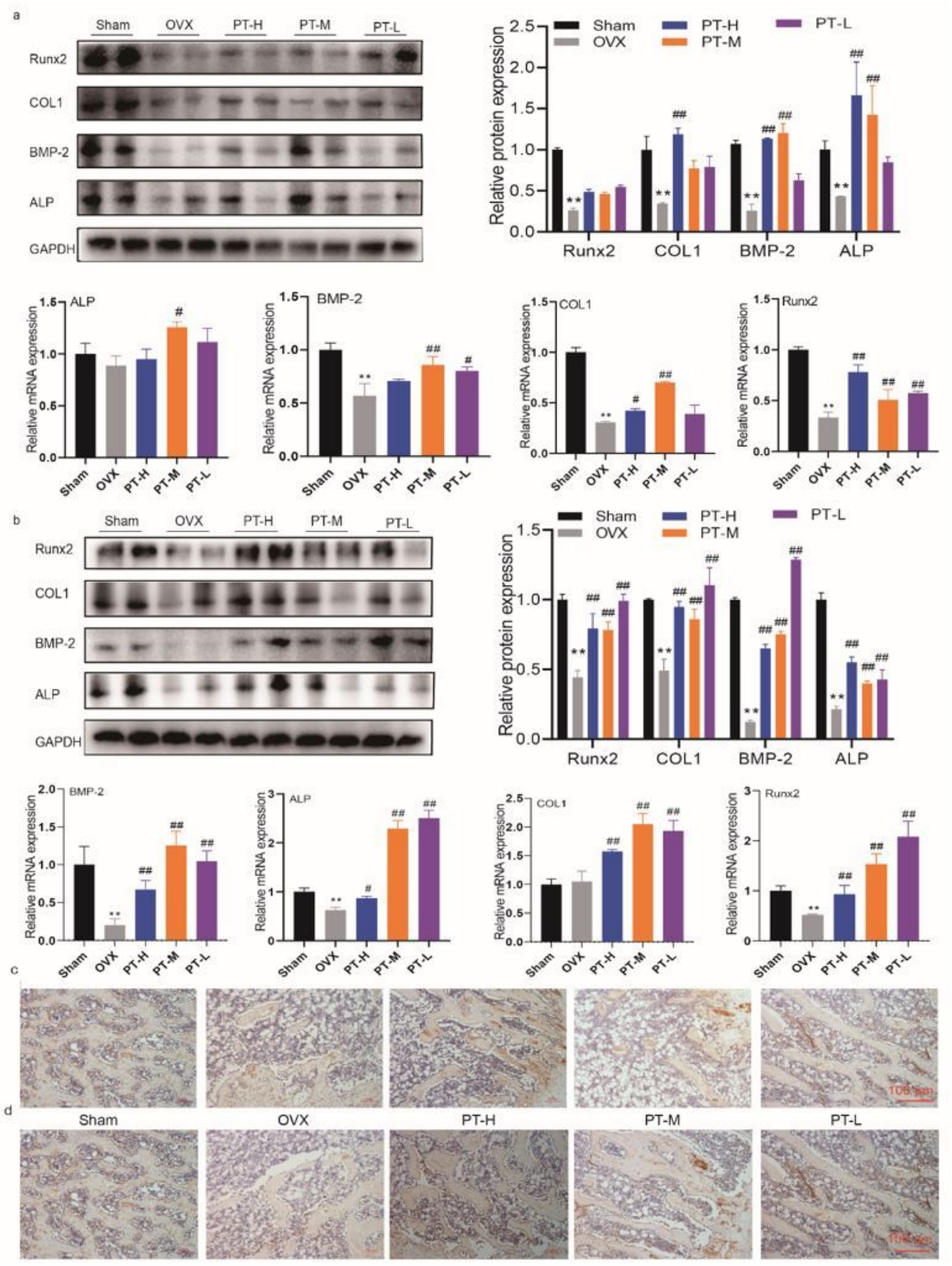

Figure 4

PT stimulated the expression of osteogenic differentiation-related factors. (a) Protein and mRNA expression of osteogenic differentiation-related factors in the femur; (b) protein and mRNA expression of

osteogenic differentiation-related factors in the lumbar vertebrae; (c) IHC staining of COL1A1 in the femur, scale bar: 100 μm; (d) IHC staining of COL1A1 in the lumbar vertebrae, scale bar: 100 μm. $^{**}P < 0.01$ vs Sham, $^{\#}P < 0.05$ vs OVX, $^{\#\#}P < 0.01$ vs OVX, analyses were performed twice and comparable results were obtained.

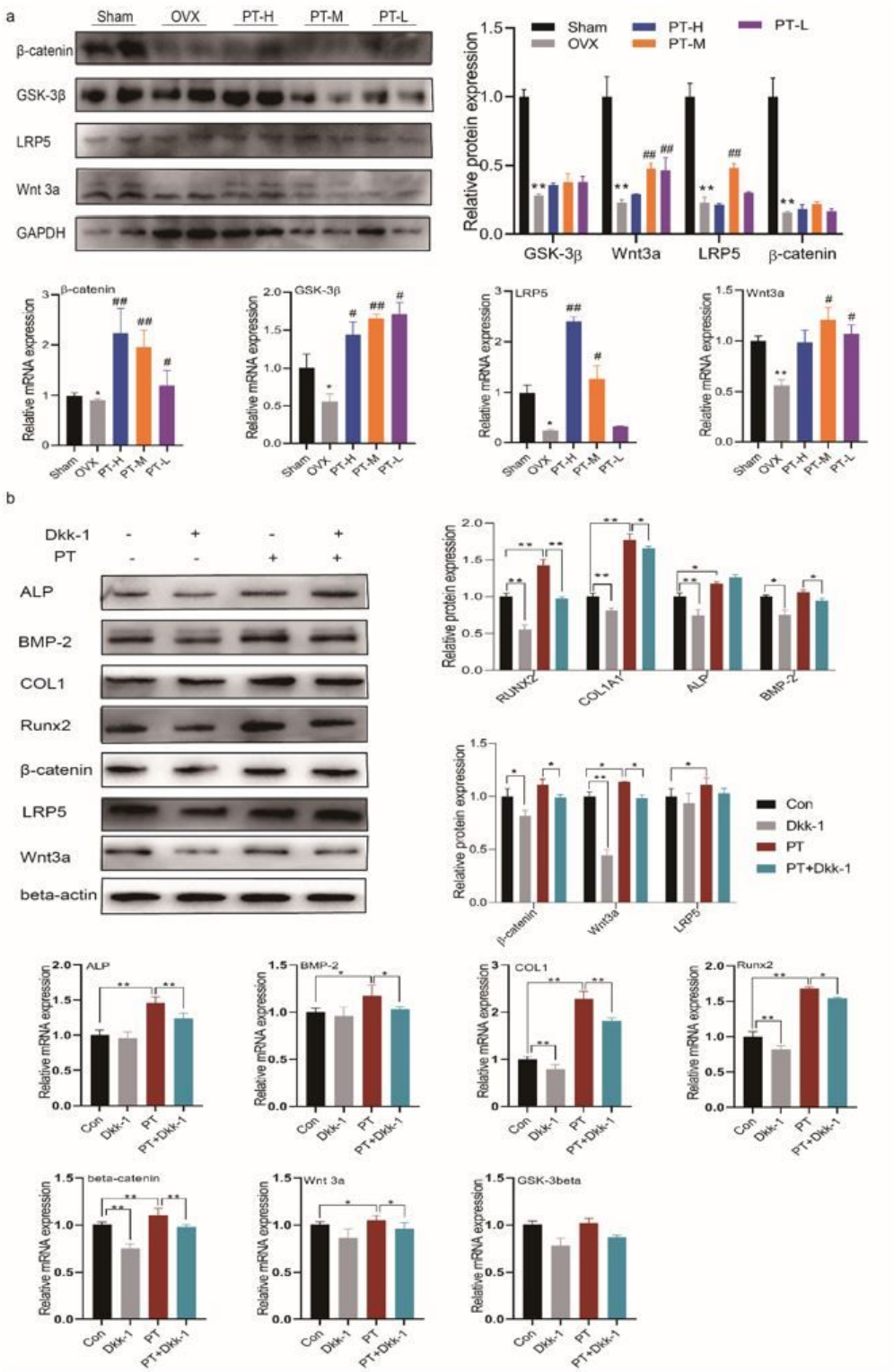

Figure 5

PT promoted osteogenic differentiation through Wnt/β-catenin signaling in BMSCs. (a) The raw data are presented as the expression of Wnt signaling-related factors in the bone tissue as mean ± SD; (b) the effect of Dkk-1 or PT on expression of Wnt signaling-related factors in BMSCs are presented as mean ± SD. $^{**}P < 0.01$ vs Sham, $^{\#}P < 0.05$ vs OVX, $^{\#\#}P < 0.01$ vs OVX; analyses were performed twice and comparable results were obtained.

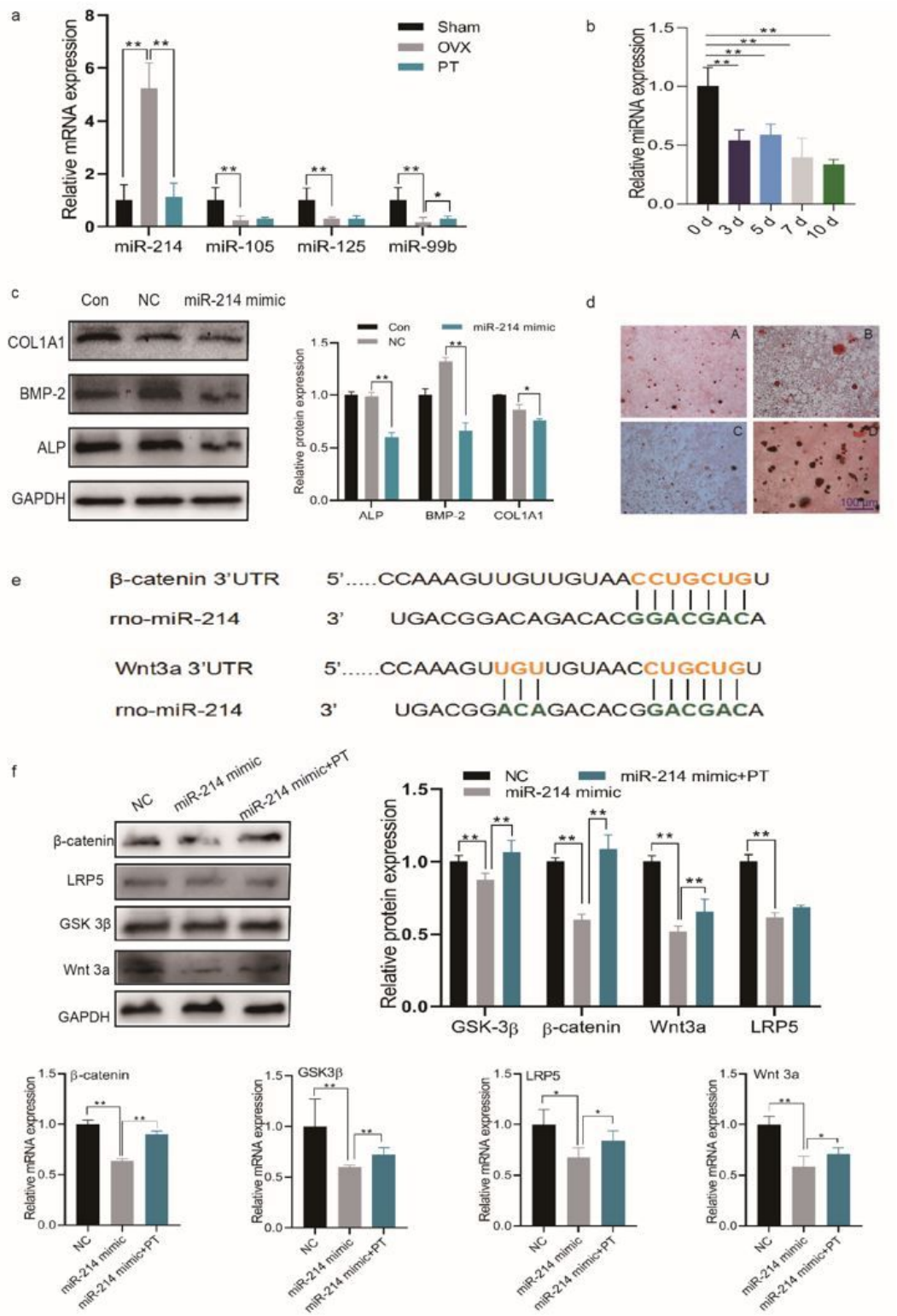

Figure 6

PT mediated miR-214 regulation of Wnt signaling to control osteogenesis. (a) Expression of miR-214 in bone tissue, raw data are represented as mean ± SD; (b) expression of miRNA under osteogenic induction conditions, the raw data are represented as mean ± SD; (c) expression of osteogenic differentiation-related factors following transfection of the miR-214 mimic, the raw data are represented as mean ± SD; (d) alizarin red S staining, scale bar: 100 μm; (e) expression of Wnt signaling-related factors following treatment with miR-214 or PT. *$P < 0.05$ vs NC, **$P < 0.01$ vs NC, analyses were performed twice and comparable results were obtained.

Supplementary Files

This is a list of supplementary files associated with this preprint. Click to download.

- GA.jpg